ELSEVIER

Journal of Nuclear Materials 273 (1999) 277–284

journal of nuclear materials

www.elsevier.nl/locate/jnucmat

Depth distribution of deuterium atoms and molecules in beryllium oxide implanted with deuterium ions

V.Kh. Alimov *, V.N. Chernikov

Institute of Physical Chemistry, Russian Academy of Sciences, Leninsky prospect 31, 117915 Moscow, Russian Federation

Received 22 October 1998; accepted 15 February 1999

Abstract

In-depth concentration profiles of deuterium (D) in beryllium oxide (BeO) films implanted with 3 keV D ions at 300 and 700 K have been determined using SIMS and RGA (residual gas analysis) measurements in the course of surface sputtering. The microstructure of implanted specimens was studied by TEM. Implanted D is found to be retained in the BeO matrix in the form of D atoms and D_2 molecules. At 300 and 700 K, the maximum concentration of deuterium in both states reaches values of 0.2 and 0.07 D/BeO, respectively. Irradiation with D ions at 300 and 700 K leads to the formation of tiny D_2 bubbles of 0.6–0.7 nm radius and of high volume density $\approx(4–5) \times 10^{24}$ m^{-3}. These bubbles together with the intercrystalline gaps are responsible for the accumulation of D_2 molecules. At both irradiation temperatures, D_2 concentration reaches in the ion stopping zone its maximum of 0.01 molecules/BeO. At 300 and 700 K, the major part of deuterium implanted in BeO films is present in the form of D atoms, probably chemically bound to O atoms. Maximum D atom concentration is 0.18 D atoms/BeO for 300 K and 0.05 D atoms/BeO for 700 K.

1. Introduction

Present concepts for ITER consider beryllium as a candidate material for the plasma-facing component of the first-wall system [1]. Sputtering of Be tiles with hydrogen isotope ions and neutrals as well as by impurity atoms leads to codeposition of beryllium, carbon, oxygen and hydrogen isotope atoms at deposition-dominated areas of the wall [2–4]. Due to a high affinity of Be to oxygen [5], beryllium oxide formation takes place. Reliable data on the hydrogen behavior in beryllium oxide, in particular, under irradiation are of great importance for the application of Be tiles in fusion devices. The database on the hydrogen behavior in BeO is very poor.

A wide range of values for the tritium diffusivity were observed by Fowler et al. [6] in studies of single crystal, sintered and powdered BeO with activation energies ranging from 0.7 to 2.3 eV. The value for the T diffusivity in sintered BeO, $D = 7 \times 10^{-6} \exp(-2.1 \text{ eV/kT})$ m^2/s, which was determined for the temperature range 923–1473 K [6], is generally used for BeO films thermally grown onto a Be substrate. The solubility of deuterium in BeO was determined to be $S \approx 10^{18} \exp(-0.8 \text{ eV/kT})$ at. m^{-3} $Pa^{-0.5}$ [7]. The solubility seems to be related to the formation of hydroxide bonds, because of the similarity of the activation energy, 0.8 eV, to the O–H bond formation energy of 0.81 eV [8].

In the close-packed hexagonal (cph) lattice of beryllium oxide, for each oxygen anion O^{2-}, 0.132 nm in radius, there are two tetrahedral interstitial sites ($r_t = 0.22r(O^{2-}) = 0.029$ nm) and one octahedral interstitial site ($r_o = 0.41r(O^{2-}) = 0.054$ nm). One of the tetrahedral interstitial sites is occupied by a beryllium cation Be^{2+} of 0.034 nm radius. The position of hydrogen in BeO can be different. Taking into account the size of a hydrogen atom (atomic radius = 0.078 nm, covalent radius = 0.03 nm) the most probable place for the hydrogen location in the non-charged state is the octahedral interstitial site. Nevertheless, the probability that hydrogen can reside in the empty tetrahedral interstitial site of the anion sublattice or in a cation vacancy (which

* Corresponding author. Tel.: +7-095 330 2192; fax: +7-095 334 8531; e-mail: alimov@ipcras.msk.ru

0022-3115/99/$ – see front matter
PII: S0022-3115(99)00054-9

is also a tetrahedral site) must not be ruled out. It is quite reasonable to suppose that hydrogen is charged positively in a cation vacancy.

The experiments on hydrogen absorption by BeO exposed to a hydrogen atmosphere [9] have revealed that the hydrogen uptake is not observed below 573 K and that at 573–773 K the hydrogen sorption is not reproducible. The H atom sorption leads to some electron transfer process detected by means of infrared spectroscopic techniques. The H sorption may have produced a chemisorbed protonic species of the type postulated on ZnO [10]. Under subsequent heating, the H species are partly or wholly desorbed as water, possibly causing the formation of anion vacancies [9].

It is suggested [8] that hydrogen atoms may react with beryllium oxide to form beryllium hydroxide by the chemical reaction

$$2BeO + 2H \rightarrow Be(OH)_2 + Be, \quad (1)$$

the STP formation energy of which is about -0.8 eV [11]. The decomposition of beryllium hydroxide is carried out according to the following reaction

$$2Be(OH)_2 \rightarrow 2BeO + H_2O \quad (2)$$

with an activation energy of 61.5 kJ/mol (0.64 eV) [12].

The trapping of ion implanted deuterium (5 keV D^+) in thermally grown BeO films at implant temperatures ranging from 140 to 470 K was investigated by Behrisch et al. [13] using the $D(^3He,H)^4He$ nuclear reaction. The ratio of implanted D to BeO molecules obtained at saturation was found to be 0.34 and 0.24 for implant temperatures of 140 and 300–470 K, respectively.

The aims of this work consisted in obtaining information on the evolution of concentration profiles of D atoms and D_2 molecules in BeO films implanted with 3 keV D ions at 300 and 700 K and the near-surface microstructure of BeO implanted with D ions.

2. Experimental

S-65B type beryllium (Brush Wellman), a powder metallurgy product that is vacuum hot pressed, containing about 1% of BeO, was used as a substrate for the formation of BeO layers.

2.1. Deuterium depth profiling

Be sample substrates were plates 8×8 mm^2 of 1 mm in thickness prepared by mechanical polishing and then electropolishing. The formation of beryllium oxide layers was done by annealing of Be electropolished plates at 1023 K for 60 min in air atmosphere at a pressure of 0.5 kPa. The thickness of the BeO layer seems to be uniform and, according to both an estimation by electron probe microanalysis and an evaluation by the weight gain, is 120 ± 20 nm.

D ion implantation and depth profile measurement were performed in a special two-chamber UHV system with a typical background pressure lower than 1×10^{-7} Pa; this pressure was mainly due to hydrogen and carbon monoxide with a small amount of water. BeO layers thermally grown onto Be substrates (BeO/Be samples) were implanted in the first vacuum chamber with mass-separated 6 keV D_2^+ ions at two temperatures, $T_{irr} = 300$ and 700 K up to fluences, Φ, in the range from 2.2×10^{19} to 6.7×10^{22} D/m^2.

After implantation, the BeO/Be samples were transferred in vacuo into the second analytical chamber for SIMS measurements of H^- and D^- secondary ion yields and RGA measurements of the partial pressures of D_2 and HD molecules in the course of sputtering of the surface with 4 keV Ar ions [14,15]. All measurements were made at 300 K, 22–24 h after ion implantation. The use of two quadrupole mass spectrometers (QMS) made it possible to register SIMS and RGA signals simultaneously. Partial pressures of HD and D_2 molecules evolved were determined taking into account the background intensities of masses 3 and 4, which were measured with the Ar ion beam switched off. The sputtering rate of the BeO layer was estimated with an accuracy of 30% as a ratio of the depth of a crater produced by sputtering on the surface of BeO/Be sample to the sputtering time; in doing so for beryllium the sputtering rate determined in Ref. [15] was taken into account. It should be noted that the sputtering rate of BeO is less than that of Be by about 20%.

We attribute the appearance of the SIMS D^- signal to the existence of separate D atoms within the matrix [15]. When recording D atom depth profiles, a special method was undertaken to minimize the influence of positive charging of the non-conductive BeO layer surface (due to Ar ion bombardment) on the D^- yield. It consisted in the simultaneous monitoring of the D^-/H^- signal ratio, as a correction factor to the experimental D^- yield. The underlying assumption is that thermal oxidation of Be in the presence of H_2O vapors is accompanied by a substantial increase of the protium concentration in BeO films (up to $\approx$0.01 H/BeO) [16] and the protium yield from BeO is constant during sputtering at constant parameters of the Ar ion beam.

Due to the recombination of sputtered D atoms with H atoms adsorbed on the inner surfaces of the vacuum chamber, the dependencies of the HD RGA signal on the depth are reminiscent of those of the D^- SIMS signal. A cause of the D_2 signal appearance seems to be the recombination of D atoms as well as the direct release of D_2 molecules from the sputtered layers. In order to distinguish the recombination and molecular fractions, the HD and D_2 RGA signals were measured simultaneously. We assume that in the absence of the molecular

fraction, the intensity of the D_2 signal should be proportional to the square of the intensity of the HD signal. Such a proportionality was observed in fact after D ion irradiation of graphite and beryllium at 300 K up to $\Phi < 1 \times 10^{20}$ D/m^2 [14,15]. In those experiments the coefficients of the proportionality, K, which depended mainly on vacuum conditions were equal in value with an accuracy of about 10%. Taking the value of K determined in the previous measurements and regarding it as a constant during sputtering in the RGA measurements, one can determine the intensity of the signal I_{mol} caused solely by the release of molecular deuterium:

$$I_{mol} = I_{D_2} - K(I_{HD})^2, \quad (3)$$

where I_{D_2} and I_{HD} are the experimentally measured intensities of the D_2 and HD RGA signals, respectively. The scale factor of D_2 concentration to RGA mass 4 intensity was estimated taking into account the sensitivity of RGA QMS and known sputtering rate and pumping speed. The total error of RGA QMS calibration was about 40%.

The D atom concentration was determined by comparison of the integral SIMS signal (all over the implantation depth) with the total amount of deuterium in the samples implanted at 300 K to low Φ (up to 6.7×10^{19} D/m^2) minus the molecular fraction. It should be noted that for the above fluences, BeO retains 100% of the implanted atoms [13].

2.2. TEM studies

BeO films about 90 nm in thickness were grown by annealing electropolished thin (200–220 μm) Be plates at 1023 K for 40 min in air atmosphere at a pressure of 0.5 kPa.

The BeO/Be samples were implanted with 2 keV D ions up to the fluence, $\Phi = 2 \times 10^{21}$ D/m^2 at 300 and 700 K. The following parameters for 2 keV D ions implanted into BeO have been adopted: the mean ion projected range $R_p = 37$ nm, the ion longitudinal straggling $\Delta R_p = 12$ nm, the maximum ion projected range $R_p^{max} = 60$ nm and the maximum range of displacement damage $R_d^{max} = 50$ nm.

A detailed description of the preparation technique for the visualization in TEM of the microstructure within the oxide layers thermally grown onto Be samples is similar to that described in Ref. [17]. Namely, these samples have been subjected to electrolytic back-thinning from the side opposite to that bearing the BeO layer designated for the investigations. The specimens prepared from thermally oxidized samples (both before and after ion implantation) were investigated in an analytical TEM (Philips EM 400T) operated at 120 kV. Bright field and dark field images were analyzed. Diffraction patterns were taken from a selected area measuring 0.5 or 1.0 μm in diameter. Small details, in particular D_2 bubbles, were studied using phase contrast under an underfocusing condition. Calculations of gas pressures inside bubbles were fulfilled by employing Yurichev's equation of state for hydrogen [18].

3. Results

3.1. Microstructural characterization of thermally grown BeO films

Systematic TEM studies of beryllium oxide layers thermally grown onto S-65B Be substrates (Fig. 1) have shown that these layers contain small cph-microcrystals of a size of 25–30 nm locally separated by non-interconnected gaps (channels) about 1 nm in width and about 10 nm in length. The estimated value of the free volume associated with these gaps is 7–10%.

3.2. Depth distribution of deuterium atoms and molecules in D ion implanted BeO

Depth profiles of D atoms and D_2 molecules in BeO/Be sample irradiated with 3 keV D ions at $T_{irr} = 300$ K are shown in Fig. 2. The maximum of the D atom distribution at $\Phi \leqslant 2 \times 10^{21}$ D/m^2 is at about 50 nm, while the thickness of the BeO layer is about 120 nm. With the fluence increase, the D atom concentration C_D reaches the value of about 1.3×10^{28} atoms/m^3 (0.18 D/BeO) and practically does not change thereafter (Fig. 2(a)).

At low fluences, $\Phi < 2.2 \times 10^{20}$ D/m^2, depth profiles of D_2 concentration, C_{D_2}, are characterized by a gradual decrease with depth (Fig. 2(b)). At $\Phi = 6.7 \times 10^{20}$ D/m^2, the C_{D_2} profile concurs with the ion projected range and the further fluence increase leads to broadening of C_{D_2}

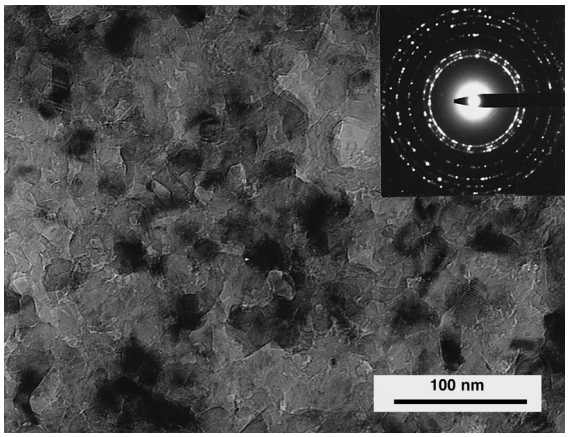

Fig. 1. Oxide film thermally grown on the surface of beryllium by annealing in air ($p_{air} = 0.5$ kPa) at 1023 K for 40 min (bright field, slightly underfocused image). In the insert is selected the area diffraction pattern related to hcp-BeO.

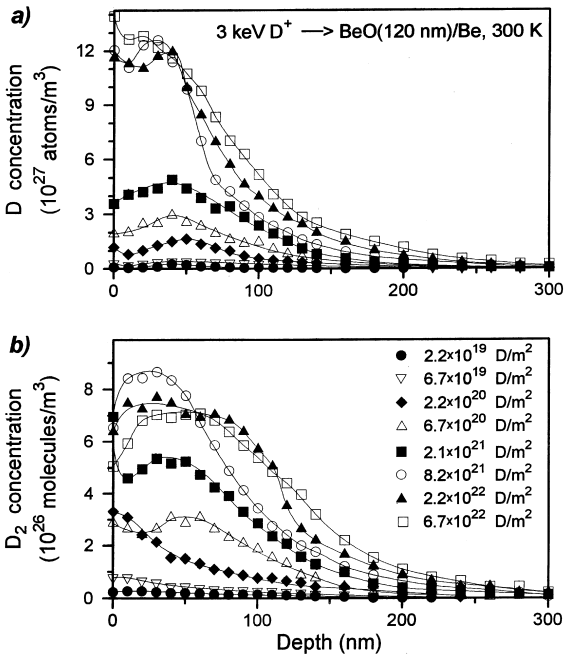

Fig. 2. Concentration profiles of deuterium trapped as D atoms (a) and in the form of D_2 molecules (b) in a 120 nm layer of BeO on the Be substrate implanted with 3 keV D ions at 300 K.

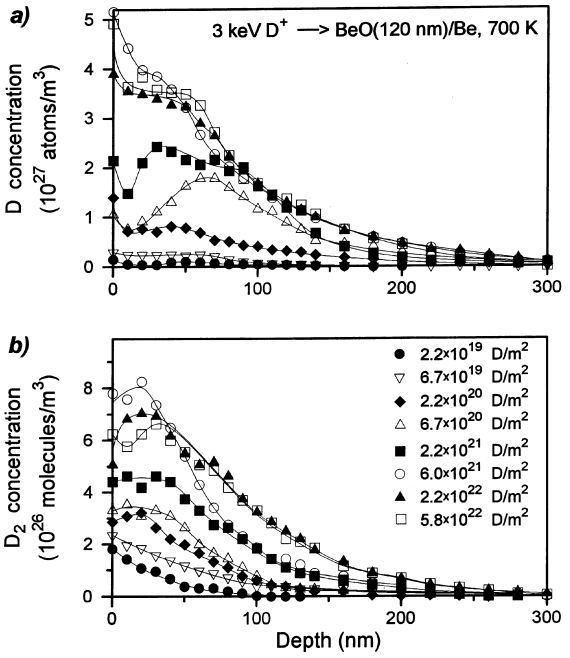

Fig. 3. Concentration profiles of deuterium trapped as D atoms (a) and in the form of D_2 molecules (b) in a 120 nm layer of BeO on Be substrate implanted with 3 keV D ions at 700 K.

profile shape. The maximum value of D_2 concentration at $T_{irr} = 300$ K is about 8×10^{26} molecules/m^3 (0.01 D_2/BeO).

As is shown in Fig. 3, the maximum concentration of D atoms reaches 4×10^{27} atoms/m^3 (0.05 D/BeO) at $T_{irr} = 700$ K. Depth profiles of D_2 molecules do not concur with the ion projected range distributions and are characterized by a gradual decrease with the depth. The maximum concentration C_{D_2} in the ion stopping zone does not exceed 8×10^{26} molecules/m^3 (0.01 D_2/BeO).

For $T_{irr} = 300$ K, the total amount of deuterium retained as atoms within the BeO film of ≈120 nm thickness and adjacent metal layers (D atom areal density) increases linearly with fluence, and reaches a value of about 1.4×10^{21} atoms/m^2 at $\Phi \approx 1 \times 10^{23}$ D/m^2, whereas the saturated amount of D_2 molecules in these layers is 1×10^{20} molecules/m^2. For $T_{irr} = 700$ K, the saturated areal densities of D atoms and D_2 molecules are 4.2×10^{20} atoms/m^2 and 0.8×10^{20} molecules/m^2, respectively (Fig. 4). Hence, the increase of the irradiation temperature from 300 to 700 K leads to the decrease in the D atom concentration by a factor of about 3 without marked change in the D_2 content.

At $T_{irr} = 300$ K, the maximum concentration of deuterium present in both states (D atoms and D_2 molecules) in the BeO layer is estimated to be about 0.2 D/BeO. This value correlates well with that reported in Ref. [13] where the ratio of D atoms to BeO molecules was found to be 0.24. After the ion implantation at $T_{irr} = 700$ K, the maximum total concentration of deuterium atoms and molecules in the ion stopping zone was estimated to be ≈0.07 D/BeO. It is pertinent to note that a similar three-fold decrease of the amount of deuterium in oxidized Be pre-implanted with 1 keV D

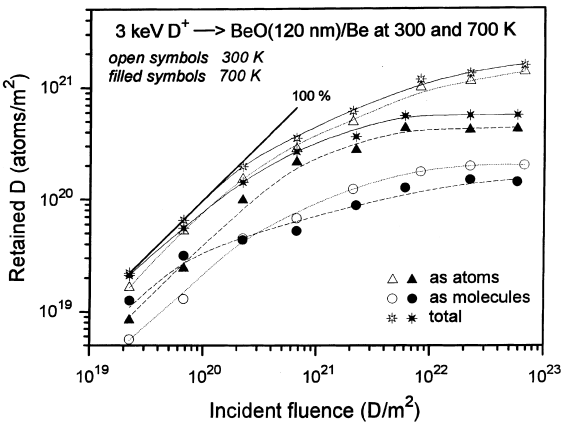

Fig. 4. Quantities of deuterium trapped as D atoms and D_2 molecules and the total amount of deuterium within the BeO film about 120 nm in thickness and adjacent metal layers implanted with 3 keV D ions at 300 and 700 K as a function of fluence. The lines are drawn to guide the eye.

ions at 300 K to saturation was observed by Möller et al. after sample heating up to 700 K [19].

3.3. Microstructure of thermally grown BeO films after D ion irradiation

After D ion irradiation at $T_{irr} = 300$ K, ion-induced defects were revealed within the oxide layer by TEM. Firstly, there is a high volume density of tiny round cavities which is illustrated in Fig. 5. Taking into consideration the presence of D_2 molecules in D implanted BeO, we have concluded that these cavities were D_2 filled bubbles. Secondly, a slight smearing of BeO diffraction rings on selected area diffraction patterns (cp. inserts in Figs. 5 and 1) provide evidence about noticeable modifications on the atomic scale. Their origin can be radiation-induced point defects and their complexes invisible in TEM together with internal stresses within the oxide due to these defects. Thirdly, some changes in the appearance of a gap network take place, namely, curing of a part of the as-grown gaps (under the action of radiation-induced stresses) and widening of some of the remaining gaps (presumably under the action of accumulated deuterium).

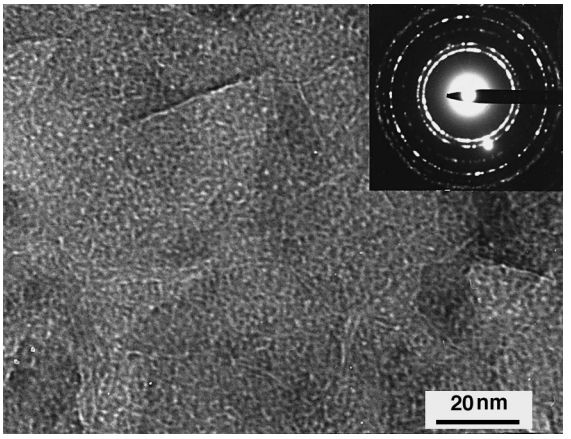

Fig. 5. Deuterium bubbles in thermally grown BeO layer after irradiation with 2 keV D ions at 300 K to $\Phi = 2 \times 10^{21}$ D/m^2 (underfocused image). In the insert is selected the area diffraction pattern of the ion damaged BeO layer.

A condition necessary for the deuterium bubble formation in BeO (along with the requirement of low gas solubility) is a displacement damage production. It means that the formation of bubbles can only proceed in the near-surface layer with a thickness of about 50 nm.

The experimentally measured parameters of deuterium bubbles, namely, mean radius r_b, volume density c_b and gas swelling due to gas bubbles $S = \Delta V/V^b$ averaged over a number of micrographs, each containing 200–250 bubbles, are listed in Table 1.

The microstructure of BeO layers subjected to D ion implantation at $T_{irr} = 700$ K, as it is evidenced by TEM, is visually indistinguishable from that of BeO layers irradiated at 300 K. Also at 700 K, very small D_2 bubbles are formed. The parameters of gas bubbles are practically identical to those observed for the case of $T_{irr} = 300$ K (Table 1). At the same time, one establishes a slight increase of the r_b value for 700 K over that for 300 K with a high degree of confidence. No striking differences are found in the appearance of intercrystalline gaps when comparing TEM micrographs of specimens irradiated at $T_{irr} = 300$ and 700 K.

4. Discussion

Whereas the depth profiles of D atoms at $T_{irr} = 300$ K are roughly described by the distribution of the ion projected range, D_2 profiles at fluences below 2×10^{20} D/m^2 are thought to be consistent with the distribution of damages generated in BeO lattice mainly due to inelastic interaction of moving D particles with electrons of oxygen anions. The anion and cation vacancies (F-centers and V_1-centers, respectively) are formed as a

Table 1
Deuterium bubble parameters and calculated concentrations of D_2 molecules in BeO implanted with 2 keV D ions to a fluence of 2×10^{21} D/m^2

	Implantation temperature, T_{irr}	
	300 K	700 K
Mean radius of bubbles, r_b (nm)	0.6	0.7
Volume density of bubbles, c_b (m^{-3})	5×10^{24}	4×10^{24}
Gas swelling due to D_2 bubbles, S (%)	0.5	0.6
Inner gas pressure in bubbles, p_g (GPa)	12.5	10.7
Concentration of D_2 molecules in bubbles, C^b_{D2} (molecules/m^3), (D_2/BeO)	5.3×10^{26}, 7.3×10^{-3}	5.7×10^{26}, 7.8×10^{-3}
Maximum concentration of D_2 molecules in gaps, C^g_{D2} (molecules/m^3), (D_2/BeO)	2×10^{26}, 2.7×10^{-3}	0.9×10^{26}, 1.2×10^{-3}
Concentration of D atoms trapped in unresolved defects, C^{pd}_D (atoms/m^3), (D/BeO) *	6×10^{27}, 8×10^{-2}	3×10^{27}, 4×10^{-2}

* Measured by SIMS/RGA method for BeO implanted with 3 keV D ions to a fluence of 3×10^{21} D/m^2.

result of the irradiation. The neutral V_1F-centers are probably served as the pore nuclei and the traps for molecular deuterium at low D ion fluences. The fluence increase leads to the deuterium bubble formation at the depth of the ion projected range, and shape of D_2 depth profiles changes – becoming Gaussian-like at a fluence of 6.7×10^{20} D/m^2. Comparison of concentration profiles of atomic and molecular deuterium in BeO allows one to estimate a minimum concentration of separate D atoms in the matrix sufficient for the onset of the appearance of D_2 gas bubbles. It is about 3 at.%. As for metallic Be irradiated with D ions, first D_2 bubbles appear at a D atom concentration of about 1 at.% [17].

The uniform distribution of deuterium in the BeO film at high fluences cannot be understood from diffusion measurements of hydrogen isotopes in BeO at very low concentrations (below 10^{-4} at.%) [6]. It is reasonable to suggest that a concentration-induced migration of D atoms takes place out from the lattice saturated with deuterium.

For making calculations concerning molecular deuterium within the bubbles, it has been assumed that all the bubbles observed in TEM are equilibrium ones, that is, their inner gas pressure, p_g, is equal to the equilibrium value $p_g^e = 2\gamma_{BeO}/r_b$, where γ_{BeO} is the specific surface energy of the BeO matrix, and they are uniformly distributed within a surface layer having a thickness of 50 nm. According to Ref. [20] γ_{BeO} exceeds 1.42 J/m^2. We estimated the value of γ_{BeO} roughly from the following simple and physically transparent equation:

$$\gamma_{BeO} \approx \frac{1}{5}\frac{E^{sb}_{BeO} \times N^{s}_{BeO}}{N_A}, \tag{4}$$

where E^{sb}_{BeO} is the heat of sublimation of BeO, $N^{s}_{BeO} = 1.74 \times 10^{19}$ molecules/m^2 is the area density of BeO molecules of the beryllium oxide, $N_A = 6.02 \times 10^{23}$ mol^{-1} is the Avogadro constant. The value of E^{sb}_{BeO} is equal to 649 kJ/mol [21]. The substitution into (4) of the above quantitative data gives readily $\gamma_{BeO} \approx 3.75$ J/m^2. Generally, the γ values for ceramics and carbides of metals are known to be somewhat higher than for the relevant pure metals. For Be $\gamma_{Be} \approx 3.13$ J/m^2 [22], therefore, the use of value $\gamma_{BeO} = 3.75$ J/m^2 in our calculations is justified. The calculated bubble parameters are listed in Table 1.

Calculations of amounts of deuterium within the gaps in molecular form are hindered by lack of information on the gas pressure therein. Only very rough estimations are possible. The yield strength of BeO in tension, σ_y(BeO), is about 100 MPa [23]. The value of σ_y for thermally grown BeO layers seems to be about 5–10 times lower compared to the above standard value due to the presence of intercrystalline gaps weakening the material strength. It means that the maximum D_2 pressure in these gaps is not in excess of $\approx 0.1\sigma_y(\text{BeO}) = 10$ MPa, which corresponds to the D_2 molecule density within the gaps, $\rho_{D_2} \approx 2.4 \times 10^{27}$ molecules/m^3. Based on the value of ρ_{D_2} and the maximum value of the free volume associated with the intercrystalline gaps, $\Delta V/V^g = 0.07 - 0.10$, one gets readily a rough estimate of the maximum concentration of implanted deuterium accumulated in intercrystalline gaps in the form of D_2 molecules:

$$C^{g}_{D_2} = \rho D_2 \times \triangle V/V^g, \tag{5}$$

which gives the resultant value of about 2×10^{26} molecules/m^3 at 300 K.

It is appropriate to note that the estimated concentration of D_2 molecules accumulated within the ion stopping zone of D ion implanted BeO ($C^{b}_{D_2} + C^{g}_{D_2} \approx 7.3 \times 10^{26}$ molecules/m^3, see Table 1) is comparable with the value of experimentally measured D_2 concentration, $C^{RGA}_{D_2}$, in BeO implanted with 3 keV D ions at $T_{irr} = 300$ K to a fluence of 3×10^{21} D/m^2 ($C^{RGA}_{D_2} = (6–7) \times 10^{26}$ molecules/m^3, see Fig. 2(b)).

The experimentally measured value of the D atom concentration $C^{SIMS}_{D} \approx 6 \times 10^{27}$ atoms/m^3 (Fig. 2(b)) could be considered as a concentration of D atoms, C^{pd}_{D}, trapped at point defects and their complexes unresolved in TEM. A chemical bonding between D and O atoms adjacent to point defects in the BeO lattice and, in particular, to radiation-induced point defects seems to be very probable. The available microdiffraction is in agreement with such a conclusion.

Table 2
Maximum concentrations of D atoms, D_2 molecules and deuterium present in both states in Be [15,17] and BeO irradiated with D ions at 300 and 700 K

	Be		BeO	
	300 K	700 K	300 K	700 K
D atom concentration (D/Be)	0.02	0.01	0.18	0.05
D_2 molecule concentration (D_2/Be)	0.04	0.01	0.01	0.01
Total D concentration (D/Be)	0.10	0.03	0.20	0.07
Gas swelling, (%)	1.8	50	0.5	0.6

The concentrations of $C^{b}_{D_2}$, $C^{g}_{D_2}$ and C^{pd}_{D} for $T_{irr} = 700$ K are also presented in Table 1. It should be noted that the calculated values $(C^{b}_{D_2} + C^{g}_{D_2})$ at $T_{irr} = 300$ and 700 K are practically equal. The similar equality is observed for the values of D_2 concentrations measured after D ion irradiation at these temperatures (cp. Fig. 2(b) and Fig. 3(b)).

The comparison of the maximum concentrations of D atoms, D_2 molecules and total deuterium present in both states in Be and BeO irradiated with D ions at 300 and 700 K to high fluences is given in Table 2. (It should be noted that Table 1 presents data on deuterium bubble parameters for D ion implantation to a fluence at which the maximum deuterium concentration is not reached yet). The study of deuterium retention in beryllium [15] has shown that a high percentage of deuterium is accumulated in the form of D_2 molecules. As for BeO, the majority of implanted deuterium is retained as D atoms both at 300 and 700 K. Attention is drawn to the fact that the value of gas-induced swelling in BeO at $T_{irr} = 700$ K is two orders of magnitude less than that for Be.

5. Conclusions

Beryllium oxide layers thermally grown onto S-65B Be substrates under annealing in air at 1023 K for 40–60 min. (90–120 nm in thickness) consist of small cph-microcrystals ($d_{BeO} = 25$–30 nm) locally separated by non-interconnected gaps about 1 nm in width and about 10 nm in length which are responsible for less than ≈7% of the free volume of the oxide.

The depth concentration profiles of deuterium trapped in the 120 nm thick beryllium oxide layer were experimentally determined as separate D atoms and D_2 molecules after the implantation with 3 keV D ions at 300 and 700 K. It was shown that the majority of implanted deuterium is retained as D atoms both at 300 and 700 K. The fraction of deuterium trapped in the form of D atoms is measured to be ≈0.85 for $T_{irr} = 300$ K and ≈0.75 for $T_{irr} = 700$ K. The maximum concentration of deuterium present in both states (D atoms and D_2 molecules) in BeO irradiated with D ions at $T_{irr} = 300$ and 700 K reaches values of 0.2 D/BeO and 0.07 D/BeO, respectively.

It is shown that the irradiation of a BeO layer ≈90 nm in thickness with 2 keV D ions at $T_{irr} = 300$ and 700 K to a fluence, $\Phi = 2 \times 10^{21}$ D/m^2 leads to the formation of tiny deuterium filled bubbles of a high volume density ($r_b = 0.6$–0.7 nm, $c_b = (4$–$5) \times 10^{24}$ m^{-3}). These bubbles together with the intercrystalline gaps are thought to be responsible for the accumulation of D_2 molecules.

Most of the D atoms seem to be chemically bonded to O atoms adjacent to point defects in the BeO lattice and in particular to radiation-induced point defects which are beyond the resolution of a TEM.

Acknowledgements

The work was supported by the United States Department of Energy, under Contract LF-7292 with Sandia National Laboratories. Valuable discussion of experimental results by Prof. A.P. Zakharov and Dr. A.E. Gorodetsky is gratefully acknowledged.

References

[1] Technical basis for the ITER interim design report, cost review and safety analysis, ITER EDA Documentation Series, No. 7. IAEA, Vienna, 1995.
[2] A.P. Martinelli, R. Behrisch, A.T. Peacock, J. Nucl. Mater. 212–215 (1994) 1245.
[3] R. Behrisch, A.P. Martinelli, S. Grigull, R. Grötzschel, U. Kreissig, D. Hildebrandt, W. Schneider, J. Nucl. Mater. 220–222 (1995) 590.
[4] M. Mayer, R. Behrisch, H. Plank, J. Roth, G. Dollinger, C.M. Frey, J. Nucl. Mater. 230 (1996) 67.
[5] K.L. Wilson, R.A. Causey, W.L. Hsu, B.E. Mills, M.F. Smith, J.B. Whitley, J. Vac. Sci. Technol. A 8 (1990) 1750.
[6] J.D. Fowler, D. Chandra, T.S. Elleman, A.W. Payne, K. Verghese, J. Am. Ceram. Soc. 60 (1977) 155.
[7] R.G. Macaulay-Newcombe, D.A. Thompson, J. Nucl. Mater. 212–215 (1992) 942.
[8] M.C. Billone, M. Dalle Donne, R.G. Macaulay-Newcombe, Fusion Eng. Des. 27 (1995) 179.
[9] M.J.D. Low, N. Ramasubramanian, J. Phys. Chem. 70 (1966) 933.
[10] R.P. Eischens, W.A. Pliskin, M.J.D. Low, J. Catalysis 1 (1962) 180.
[11] M.W. Chase Jr., C.A. Davies, J.R. Downey Jr., D.J. Frurip, R.A. McDonald, A.N. Syverud, JANAF thermochemical tables, 3rd ed., Part I, aluminium–cobalt, J. Phys. Chem. Ref. Data (Suppl. 14) (1985) 1.
[12] D.T. Livey, J. Williams, Proc. Second UN International Conference on Peaceful Uses of Atomic Energy Geneva, vol. 5, 1958, 311.
[13] R. Behrisch, R.S. Blewer, J. Borders, R. Langley, J. Roth, B.M.U. Scherzer, R. Schulz, Radiat. Eff. 48 (1980) 221.
[14] V.Kh. Alimov, A.E. Gorodetsky, A.P. Zakharov, J. Nucl. Mater. 186 (1991) 27.
[15] V.Kh. Alimov, V.N. Chernikov, A.P. Zakharov, J. Nucl. Mater. 241–243 (1997) 1047.
[16] I.I. Papirov, Oxidation and Protection of Beryllium, Moscow, Metallurgiya, 1968 (in Russian).
[17] V.N. Chernikov, V.Kh. Alimov, A.V. Markin, A.P. Zakharov, J. Nucl. Mater. 228 (1996) 47.
[18] I.A. Yurichev, Teplofizika (in Russian) 17 (1979) 1187.
[19] W. Möller, B.M.U. Scherzer, J. Bohdansky, IPP-JET Report No. 26, Max-Planck-Institut für Plasmaphysik, Garching, 1985.
[20] D.T. Livey, P.J. Murray, J. Am. Ceram. Soc. 39 (1956) 363.
[21] R.A. Beliaev, Beryllium Oxide, Moscow, Gosatomizdat, 1962 (in Russian).
[22] M. Dalle Donne, F. Scaffidi-Argentina, C. Ferrero, C. Ronchi, J. Nucl. Mater. 212–215 (1994) 954.

[23] G.V. Samsonov, T.G. Bulankova, A.L. Burykina, T.N. Znatokova, Yu.P. Kaloshina, A.F. Kiseleva, P.S. Kisly, M.S. Koval'chenko, T.Ya. Kosolapova, Ya.S. Malakhov, A.D. Panasyuk, R.M. Sannikova, N.I. Tkachenko, Physical and Chemical Properties of Oxides, Reference Book, Moscow, Metallurgia, 1969, p. 237 (in Russian).